Cell Reports

Resource

Single Muscle Fiber Proteomics Reveals Fiber-Type-Specific Features of Human Muscle Aging

Graphical Abstract

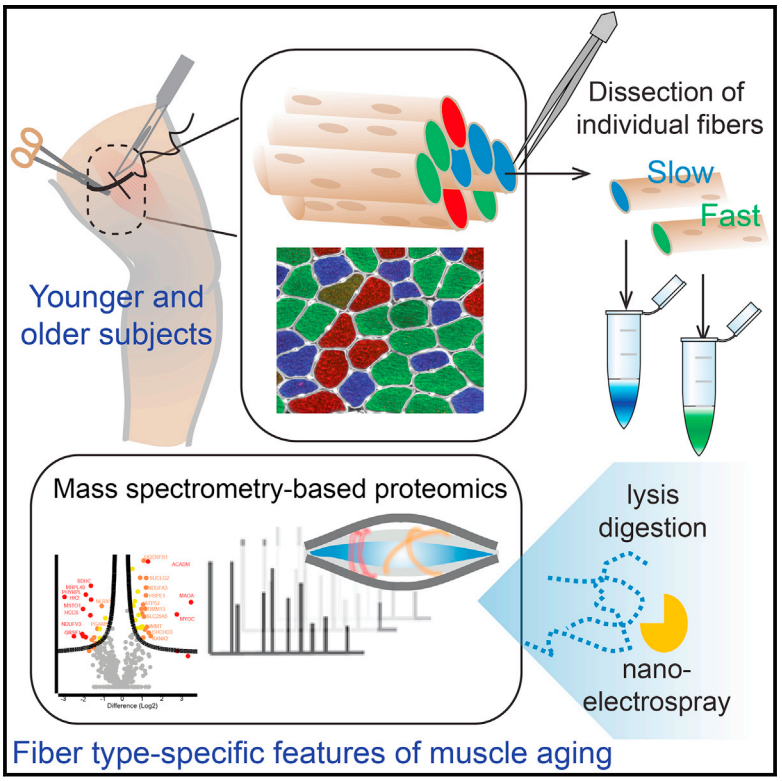

Authors

Marta Murgia, Luana Toniolo, Nagarjuna Nagaraj, ..., Stefano Schiaffino, Carlo Reggiani, Matthias Mann

Correspondence

mmurgia@biochem.mpg.de (M.M.), mmann@biochem.mpg.de (M.M.)

In Brief

Murgia et al. use mass-spectrometry-based proteomics to compare single muscle fibers of younger and older subjects, which revealed that glycolysis and glycogen metabolism decrease strongly in aging fast, but not slow, muscle fibers. The proteomic changes revealed here help to explain differential loss of muscle performance in aging.

Highlights

- Single-fiber proteomic analysis of human muscle aging
- Oxidative phosphorylation decreases similarly in slow and fast fibers
- Enzymes of carbohydrate metabolism increase in slow and decrease in fast aging fibers
- Proteomics elucidates why fast fibers age more rapidly than slow ones

Accession Numbers

PXD006182

Murgia et al., 2017, Cell Reports *19*, 2396–2409
June 13, 2017
http://dx.doi.org/10.1016/j.celrep.2017.05.054

CellPress

OPEN ACCESS
CellPress

Cell Reports
Resource

Single Muscle Fiber Proteomics Reveals Fiber-Type-Specific Features of Human Muscle Aging

Marta Murgia,[1,2,*] Luana Toniolo,[2] Nagarjuna Nagaraj,[1] Stefano Ciciliot,[3,4] Vincenzo Vindigni,[5] Stefano Schiaffino,[3] Carlo Reggiani,[2] and Matthias Mann[1,6,*]
[1]Max-Planck-Institute of Biochemistry, Martinsried 82152, Germany
[2]Department of Biomedical Science, University of Padova, Padua 35121, Italy
[3]Venetian Institute of Molecular Medicine, Padua 35129, Italy
[4]Department of Medicine, University of Padua, Padua 35128, Italy
[5]Department of Neurosciences, University of Padova, Padua 35128, Italy
[6]Lead Contact
*Correspondence: mmurgia@biochem.mpg.de (M.M.), mmann@biochem.mpg.de (M.M.)
http://dx.doi.org/10.1016/j.celrep.2017.05.054

SUMMARY

Skeletal muscle is a key tissue in human aging, which affects different muscle fiber types unequally. We developed a highly sensitive single muscle fiber proteomics workflow to study human aging and show that the senescence of slow and fast muscle fibers is characterized by diverging metabolic and protein quality control adaptations. Whereas mitochondrial content declines with aging in both fiber types, glycolysis and glycogen metabolism are upregulated in slow but downregulated in fast muscle fibers. Aging mitochondria decrease expression of the redox enzyme monoamine oxidase A. Slow fibers upregulate a subset of actin and myosin chaperones, whereas an opposite change happens in fast fibers. These changes in metabolism and sarcomere quality control may be related to the ability of slow, but not fast, muscle fibers to maintain their mass during aging. We conclude that single muscle fiber analysis by proteomics can elucidate pathophysiology in a sub-type-specific manner.

INTRODUCTION

Skeletal muscle has a primary role in locomotion and in the maintenance of posture but also shapes metabolic homeostasis by taking up glucose and oxidizing fatty acids. Muscle fibers are multinucleated single cells responsible for this repertoire of functional tasks. There are four fiber types in mammalian muscle, slow (type 1) and three fast types (2A, 2X, and 2B), each characterized by the expression of one specific isoform of myosin heavy chain (MYH), which is the main determinant of their contractile properties. Fiber types, however, also differ in their metabolic profile, ranging from slow/oxidative to fast/glycolytic. Unlike rodent muscles, which contain different proportions of all four fiber types, human muscles lack fast 2B fibers, the fastest and most glycolytic type (Schiaffino and Reggiani, 2011).

Single muscle fibers have been isolated and studied for decades using electrophoresis to distinguish different MYH isoforms and enzymatic assays to analyze their metabolic profile (Klitgaard et al., 1990; Conjard and Pette, 1999). These pioneering studies contributed the essential basis of our current knowledge of the structure-function relationship in muscle fibers. However, each fiber only yields one or very few readouts, and a global characterization of the individual fiber phenotype has been hindered by technological limitations. Recently, a transcriptomic analysis of slow and fast 2B fiber types in the mouse model has provided a broader view of the muscle fiber phenotype at the RNA level (Chemello et al., 2011).

In a previous study, we set out to understand muscle tissue complexity directly at the level of single cellular units, building on recent advances in quantitative mass spectrometry (MS)-based proteomics (Aebersold and Mann, 2016). MS analysis of muscle tissue is challenging because of the unfavorable dynamic range caused by highly abundant sarcomeric elements (Deshmukh et al., 2015). We devised a sensitive workflow, which allowed us to obtain the proteome of single mouse muscle fibers and describe individual features of each fiber type (Murgia et al., 2015). Fiber-type-specific analysis offered an unprecedented proteomic view into the muscle tissue, which is also devoid of confounding contributions of connective tissue, blood vessels, and nerves, which are present in whole-muscle lysates. That analysis revealed that the mitochondria of different fiber types have diverging capabilities for substrate utilization.

Loss of muscle mass and strength inevitably accompany the aging process, with severe consequences on life quality. Specifically, it is a primary cause of sarcopenia—a leading cause of death in the elderly (Landi et al., 2013). Notably, this decline can at least partially be mitigated by physical activity (Cartee et al., 2016). Here, we investigated human muscle aging with our single-fiber proteomic approach. We compare single human muscle fibers from younger and older donors. Both cohorts are healthy and physically active, allowing us to focus on primary aging without confounding effects due to inactivity. Our proteomic analysis of human muscle aging at the single-fiber level reveals type-specific and even diverging changes in molecular machines and specific enzyme systems.

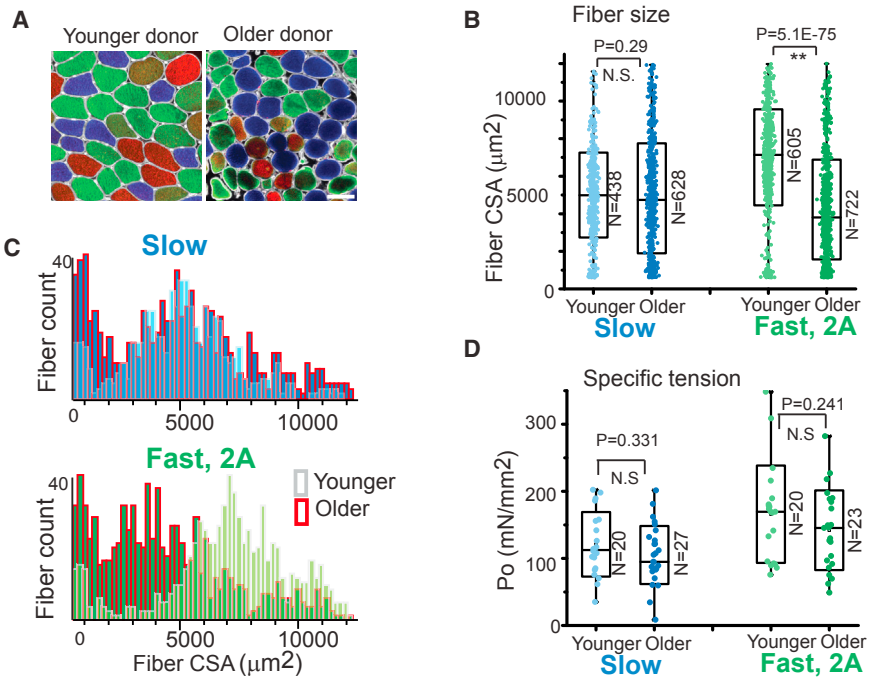

Figure 1. Morphology and Functional Analysis of Different Fiber Types from Younger and Older Donors

(A) Cross sections of muscle biopsies stained with antibodies specific for slow (anti-MYH7, blue), fast 2A (anti-MYH2, green), and fast 2X fibers (anti-MYH1, red). Representative images from one younger and one older donor are shown. The bar represents 100 μm.

(B) Fiber size (cross-sectional area [CSA]) measured in the biopsies from all younger and older donors. Slow and fast 2A fiber types were quantitated separately based on the staining shown in (A). Boxplots showing data as mean ± SD are superimposed on the individual data points. Whiskers indicate minimum and maximum values. The total number of fibers analyzed is indicated next to the bars corresponding to each subgroup. Statistical significance with corresponding p value (Student's t test) is indicated on top (N.S., not significant).

(C) Fiber size distribution of slow and fast 2A fibers. The graphs representing younger and older donors have been superimposed.

(D) Measurement of specific tension in isolated muscle fibers. The force produced by each single fiber was divided by the corresponding cross-sectional area to obtain the force produced by a given unit of muscle tissue. Data representation as in (B).

RESULTS

Morphological and Functional Analysis of Muscle Biopsies from Younger and Older Donors

To quantify the proteomic changes occurring in single human muscle fibers during aging, we obtained muscle biopsies of vastus lateralis from a cohort of eight donors representing two age groups, younger (22–27) and older (65–75). Because disease and physical inactivity account for major changes in muscle that add to the intrinsic effect of "primary aging" (Cartee et al., 2016), we ensured that all donors of both age groups were healthy and physically active (Table S1). Needle biopsies consisting of multiple fiber fascicles were obtained from all donors, allowing us to perform parallel analyses with different techniques. First, we characterized the muscle samples of each donor according to state-of-the-art procedures aimed at determining fiber size and type and the active tension developed by single fibers. Cryosections of muscle biopsies from each donor were stained with antibodies specific for the adult isoforms of myosin heavy chain (MYH).

Two representative cross sections from a younger and an older donor were stained in blue (slow type 1 fibers), green (fast 2A) and red (fast 2X; Figure 1A). The different fiber types were counted and their cross-sectional areas measured. The results of a cumulative analysis of fiber sizes comparing the younger and older cohort of donors showed no significant difference for slow fibers but a highly significant reduction of about one-third in size for fast 2A fibers ($p < 10^{-75}$; Figures 1B and S1). This is in accord with previous reports showing selective atrophy of aging fast fibers (Brunner et al., 2007; Grimby, 1995). Fast 2X fibers were not present in all donors and were rare in the older cohort. The size distribution for these fibers in older donors was clearly shifted toward smaller cross-sectional areas compared to those of the young subjects. In contrast, the fiber size distribution in younger and older slow fibers was essentially superimposable (Figure 1C).

For each of the donors, we used a separate group of single fibers from the same punch biopsy to determine the maximal isometric force and specific tension, defined as the force divided by the corresponding cross-sectional area. For these measurements, fibers are permeabilized and activated to contract at a fixed extracellular calcium concentration (Experimental Procedures). The specific tension therefore measures the force produced in a given unit of muscle mass, reflecting the intrinsic ability of the sarcomeric apparatus to undergo contraction. We then subjected the same fibers to electrophoresis to determine MYH composition and thus fiber type (Figure S2A). Our analysis did not detect significant differences in the specific tension produced by fibers from old and young donors in either fiber type (Figure 1D).

Together, the analyses of the biopsies in our cohort demonstrate atrophy of fast, but not slow, fibers in the older donors, in line with previous studies (Brunner et al., 2007; Klitgaard et al., 1990). The observation that specific tension is not affected by aging has also been made before (Deschenes, 2004; Kent-Braun and Ng, 1999) and indicates that a decrease in muscle force in aging must be predominantly due to a change in mass, with possible additional contributions from the components of excitation-contraction coupling (Payne et al., 2009). Having established a functional fiber type difference in healthy aging of human muscle, we then wished to characterize the proteome remodeling underlying this process.

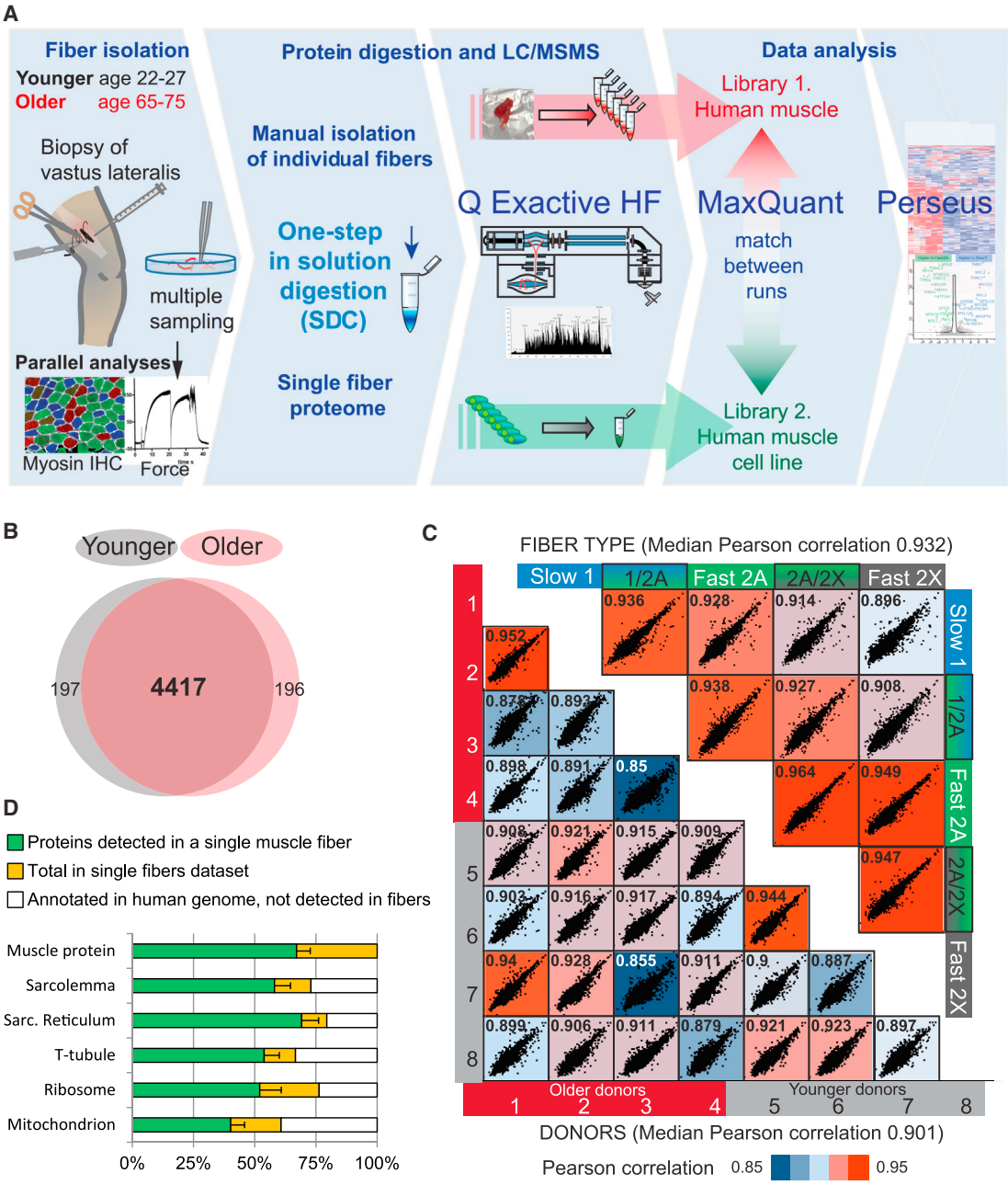

Figure 2. Characterization of the Proteome of Human Muscle Fibers from Biopsies of Vastus Lateralis

(A) Shotgun proteomics workflow for single fibers and peptide-library-based strategy.

(B) Venn diagram of quantified proteins in the two age groups.

(C) Matrix of correlations between label-free quantification (LFQ) intensities of eight donors (left) and five pure and mixed fiber types (right). Pearson correlation coefficients are reported for each comparison. The color code follows the indicated values of correlation coefficient.

(D) Protein coverage in muscle fibers. Each bar represents a selected category of keywords or GO annotations. The number of proteins quantified in a single human muscle fiber (median ± SD) is shown in green; total identifications in our fibers database correspond to green and orange bars combined. The number of corresponding protein-coding genes in the human genome (UniProt) is considered as 100%.

Quantitative Proteomics of Human Aging Muscle Fibers

We obtained the proteomes of single human muscle fibers after optimizing a workflow that we had previously devised for the murine model (Figure 2A; Experimental Procedures; Murgia et al., 2015). Briefly, we confined all sample processing and peptide purification steps to a single vessel, thus minimizing sample loss. The liquid chromatography (LC)-MS analysis of individual fibers was then performed in single-run format for maximum

sensitivity. All measurements were performed in a linear quadrupole ultra-high-field Orbitrap mass analyzer (Q Exactive HF), characterized by high sensitivity, sequencing speed, and mass accuracy (Scheltema et al., 2014). This instrument allowed us to maximize the number of peptides detected, thereby expanding the coverage of low-abundance proteins.

Another key step in the workflow established for the single-murine muscle fibers was the "match between runs" capability in the MaxQuant computational proteomics platform (Cox and Mann, 2008; Murgia et al., 2015).This feature uses accurate LC retention time alignments to convey identifications from a peptide library, which is separately established on larger amounts, making successful fragmentation and identification of low-abundance muscle peptides and proteins much more likely (Deshmukh et al., 2015). Therefore, to further increase the depth of proteomic analysis, we obtained two deep skeletal muscle proteomes to support protein identification in single fibers. The first library was derived from the tryptic digestion of whole human muscle homogenates, followed by fractionation of the complex peptide mixtures into eight fractions using a loss-less nano-fractionator (Kulak et al., 2017). This pre-fractionation step allowed us to increase proteome coverage in skeletal muscle. For the second library, we used cultured muscle cells from human induced pluripotent stem cells. Together, the two libraries provided deep-muscle peptide (54,000) and protein identifications (6,000), as shown in Tables S2 and S3, respectively.

We applied our high-sensitivity workflow to 152 single fibers across the eight donors. This identified more than 60,000 peptides and more than 5,400 proteins, both at a false discovery rate (FDR) of 1% (Table S4; note that, compared to the library, the single fiber proteomes lack proteins from other cell types). A total of 74% of these proteins were quantified in at least six of eight donors and 84% in at least four of eight, and only 5% were unique to single donors. Almost all proteins (92%) were quantified in both the younger and older donor groups, and we obtained, on average, 2,100 proteins per single muscle fiber (Figure 2B). Our method is very robust and allowed us to obtain very stable protein quantifications throughout the entire dataset (Figure S2B).

To quantify the variability of the muscle fiber proteome among different donors, we compared median protein abundances across all individuals. We used the MaxQuant label-free quantification (LFQ) algorithm (Cox et al., 2014) to quantitate the MS signals from the same peptides in the 152 raw data files (18–20 single fibers and MS files per donor). Between different donors, median Pearson's correlation coefficients were 0.90, ranging from 0.85 to 0.95 for the least to the most similar individuals. We then compared pools of fibers from different donors assigned to each of the fiber types by MS-based detection (Murgia et al., 2015; Figure 2C). Pearson's correlation coefficients were higher, with a median of 0.93 and a maximum of 0.964 for the most similar ones, when comparing the same fiber types derived from different donors. Thus, fiber-type-specific analysis of our cohort of donors reveals that variability among individuals is outweighed by functional similarity between their fiber types.

The signal intensity of all proteins detected in the individual muscle fibers, ranked from highest to lowest abundant, spans more than seven orders of magnitude and is dominated by a few sarcomeric proteins (Figure S2C). Dividing the single-fiber proteomes into four quartiles shows an accumulation of Gene Ontology (GO) terms for sarcomeric, ribosomal, and mitochondrial proteins in the high-abundance segment, whereas categories containing low-abundance proteins, such as "chromatin," accumulate on the low side of the ranking. This analysis demonstrates good coverage of structural and metabolic features of the muscle fiber proteome, with an average identification of 60% of proteins annotated to the sarcolemma and 70% of sarcoplasmic reticulum proteins in single fibers. Even broader annotations, such as ribosome (169 proteins), are covered almost to completion in the entire single fiber set and to more than half in individual ones on average (Figure 2D).

Proteomic Features of Aging in Different Fiber Types

To assign fiber type based on proteomics, we quantitated the expression of MYH isoforms of each individual fiber analyzed by MS. Different isoforms of MYH have more than 80% sequence identity; therefore, we quantitated MYH expression exclusively by the intensities of peptides unique for each isoform (Drexler et al., 2012; Fraterman et al., 2007; Murgia et al., 2015). Ranking fibers by purity (percentage of the dominant MYH isoform) revealed that the majority of the 152 fibers, regardless of the age group, expressed predominantly one isoform of MYH (Figure 3A). Defining "pure fibers" as those expressing at least 80% of MYH as a single isoform resulted in 76% pure slow fibers and 79% pure fast fibers (Table S5).

Pure fast 2X fibers were comparatively rare, in line with the morphological results shown above, and were not represented among the pure fibers of the old donor cohort. The subset of fibers expressing more than one MYH isoform—the "mixed fibers"—could be assigned to two groups: mixed slow and fast 2A (co-expressing variable combinations of MYH7 and MYH2) and mixed fast 2A/2X (co-expressing MYH2 and MYH1; Table S3). The expression of MYH4, specific for the fastest 2B fiber type, was negligible as expected (Harrison et al., 2011). Only pure type 1 and 2A fibers, which were numerous in all donors, were systematically used in subsequent analyses.

The significant change in cross-sectional area observed only in old type 2A fibers (Figure 1B) requires additional normalization to allow comparison with the other fiber groups at the whole-proteome level. As a measure of quantities of the different proteins in the detected fiber proteomes, we use an expression value corresponding to the summed intensity of the peptides identifying each protein, divided by the number of theoretically observable peptides, which provides information on the relative abundance of identified proteins (Schwanhäusser et al., 2011; Cox et al., 2014). Because the sampled fiber segments can have different length as a result of the isolation procedure, we additionally correct the results by the expression of sarcomeric actin (ACTA1), as previously described (Murgia et al., 2015).

Correct normalization should result in roughly equal expression values of household cytoskeletal proteins, such as desmin and the plasmalemma surface protein dystroglycan (DAG). This is indeed the case after ACTA1-based normalization, whereas absence of normalization results in a systematic underestimation of the amounts of the two proteins in older fast 2A fibers. For comparison, we also normalized by the expression of DMD, which

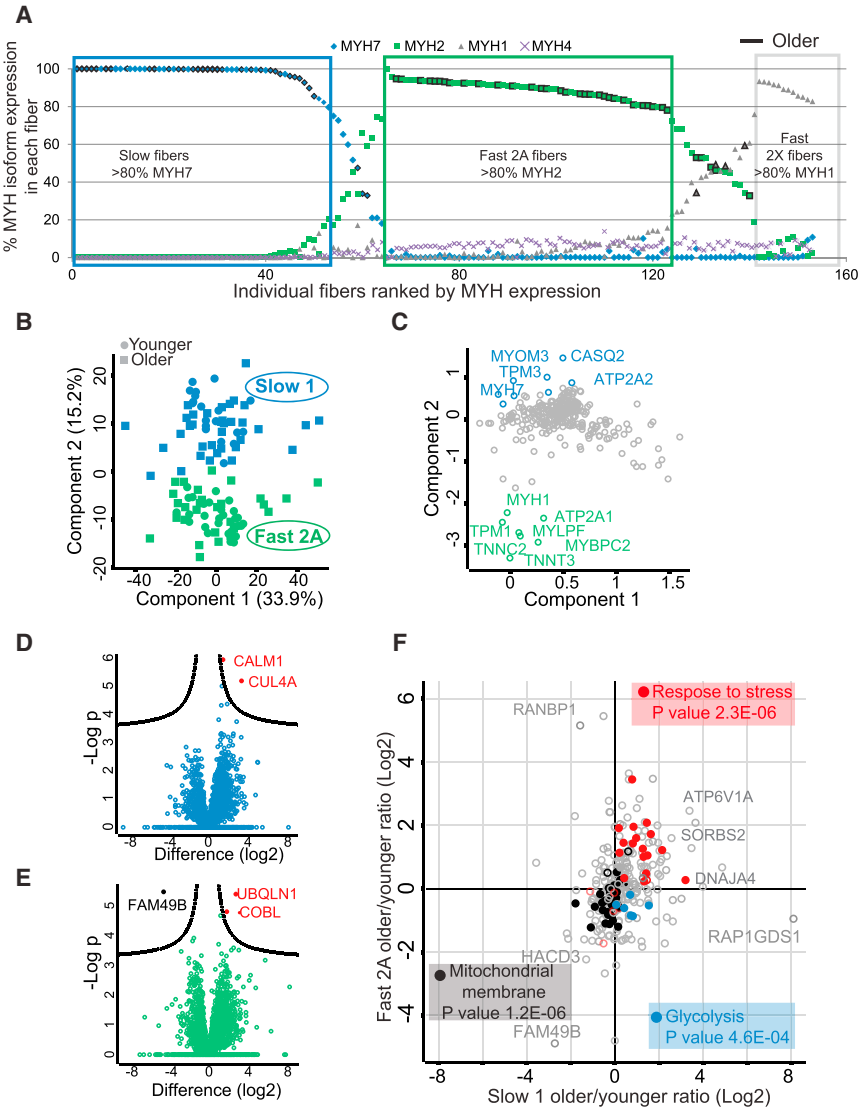

Figure 3. Features of Fiber Type and Impact of Aging Can Be Clearly Distinguished

(A) MS-based quantification of MYH isoforms reveals pure-type fibers and different combinations of mixed-type fibers. The scatter graph shows the percent expression of the four adult isoforms of MYH in all analyzed fibers, distributed along the x axis. Fibers from older donors have a black contour. Fibers were ordered and ranked based on the prevalence of expression of MYH7 (blue diamonds), MYH2 (green squares), and MYH1 (gray triangles) isoforms. MYH4 (cross) was essentially not expressed, as expected. Fibers were assigned to the indicated fiber type based on the most expressed isoform (see text and Table S3).

(B) Principal-component analysis (PCA) performed on pure slow and fast 2A fibers (n = 111). Components were derived from proteins expressed in all fibers.

(C) Loadings of the PCA in (B) showing the proteins driving segregation into components. A subset of main drivers, prominent determinants of fiber type specificity, is marked in blue and green for the two fiber types, respectively.

(D) Volcano plot of statistical significance against fold-change, highlighting the most significantly different proteins between younger and older slow fibers.

(E) Volcano plot as in (D) for fast 2A fibers.

(F) Scatterplot showing proteins differentially expressed by age and fiber type. Specific enrichments for each quadrant were calculated by Fischer's exact test, using Benjamini-Hochberg FDR for truncation and a threshold value of 0.02. All proteins corresponding to the enriched annotations are marked with filled dots of the color corresponding to the quadrant and cartoon.

also corrected the systematically lower values in older fast 2A fibers (Figure S2D), consistent with the observed lower cross-sectional area. All subsequent analyses therefore normalize by ACTA1, with normalization by DMD as a further control (for complete dataset normalized for ACTA1, see Table S6).

Principal-component analysis (PCA) yielded a separation into two groups, corresponding to type 1 and type 2A (Figure 3B). The major drivers of the PCA separation were MYH isoforms, calsequestrins and troponins, known markers of fiber type specificity (Figure 3C). This ability to clearly distinguish fiber types encouraged us to investigate potential fiber-type-specific features of aging. To this end, we grouped slow and fast 2A fibers and quantitatively compared their proteome differences. We determined statistical significance in the resulting volcano plots by permutation-based FDR. The expression of CUL4, a core component of E3 ubiquitin ligases, and of the cytosolic calcium sensor calmodulin (CALM1), is significantly higher in older slow fibers than in their younger counterparts (Figure 3D). As slow fibers do not show atrophy in our active donor cohort, higher CUL4 expression might be related to a general increase in sarcomere quality control in aging slow fibers (see below). CALM1 has not previously been implicated in muscle aging; however, dysregulation of calcium signaling is a feature of aging in other excitable tissues (Buchholz et al., 2007). The equivalent comparison in our pure subset of fast 2A fibers showed few changes, among them significantly higher expression of the FAM49B protein in young fast fibers (Figure 3E). This protein of unknown function is downregulated in patients with endometriosis (Williams et al., 2015) and pregnancy-associated multiple sclerosis (Gilli et al., 2010)—disorders associated with a strong inflammatory response. The possible role in skeletal muscle aging of FAM49B could therefore be another connection between aging and inflammation.

To investigate whether aging affects slow and fast fibers in the same way, we subdivided our dataset into four groups by pure fiber type and age (slow and younger, slow and older, fast and younger 2A, and fast and older 2A). ANOVA using 5% permutation-based FDR retrieved 313 significantly changing proteins, whose level of expression changed between at least two of the four groups. We log transformed the

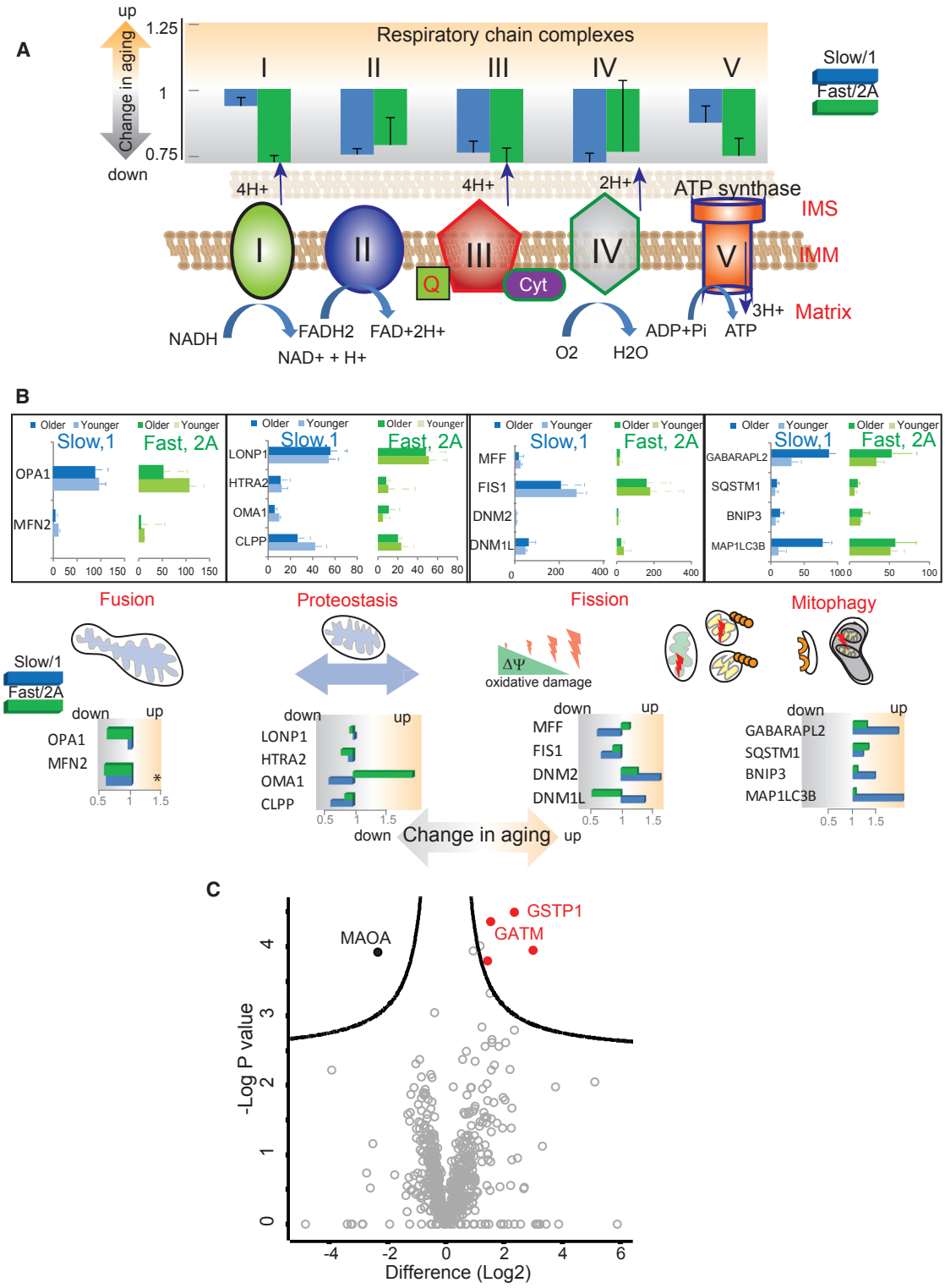

Figure 4. Features of Mitochondrial Aging in Slow and Fast Fibers

(A) The respiratory chain complexes, showing the median expression change in aging, cumulative for all proteins in each complex. Data are represented as median change ± SEM. The corresponding expression values are detailed in Figure S4. For each complex, we report the changes in slow (left, blue bar) and fast 2A fibers (right, green bar). The corresponding color scale is shown on the left.

(legend continued on next page)

older/younger ratios of these proteins in the two fiber types and compared them in a scatterplot, highlighting proteins that increase or decrease with age and proteins that differ by fiber type (Figure 3E). Fischer's exact test revealed that proteins with mitochondrial annotations were enriched in younger fibers, irrespective of fiber type (black dots). These included the above-mentioned FAM49B as well as HACD3, an enzyme involved in fatty acid elongation, both of which decreased more than 4-fold in the older group. The annotation "response to stress," was significantly enriched in the older group independent of fiber type ($p < 3 \times 10^{-6}$; red dots). In this set, we found proteins assigned to the unfolded protein response, such as ATP6V1A and DNAJA4, and regulators of the assembly of the motor endplate, such as SORBS2.

Intriguingly, the quadrant comprising proteins enriched in older slow fibers showed a significant enrichment in glycolysis using both UniProt keywords and a protein list manually curated by us. Together, our analysis of fiber-type-specific aging clearly points to fiber-specific changes in energy metabolism during muscle aging.

Decreased Respiratory Chain Complexes in Aging Muscle Fibers

Mitochondrial content and function are affected by the aging process (Lanza et al., 2005; Short et al., 2005) and increased by exercise, independent of age (Irving et al., 2015). Our dataset provides the virtually complete quantification of all five respiratory chain complexes, comprising both the nuclear- and mitochondrial-encoded subunits, and clearly shows that respiratory chain proteins are more abundant in type 1 than in type 2A fibers (Figure S3A), a known feature of human muscle (Hood et al., 2016). In both slow and fast fibers, we observed decreased expression of respiratory chain complexes, defined as "change in aging" in the figures. The decrease in complex I was modest in slow fibers (about 10%) and more pronounced in fast 2A (about 25%), whereas the decrease was uniform in both fiber types for the other four respiratory chain complexes (20%; Figure 4A). The mitochondrial content in aging muscle has been extensively studied, both with morphological techniques measuring organellar volume and enzymatic assays of the activity of the respiratory chain (reviewed in Carter et al., 2015). Despite discrepancies in reports on different muscles, possibly related to differences in workload, a decline in the mitochondrial function of older vastus lateralis has consistently been observed (Kent and Fitzgerald, 2016), in agreement with our proteomics results. Furthermore, by quantifying the expression of each element of the entire respiratory chain, we show that the decrease is similar in slow and fast fibers despite their different mitochondrial content.

Regardless of the causes of the mitochondrial decline, our dataset allows us to investigate whether the fusion-fission machinery and the quality control mechanisms responsible for the removal of non-functional mitochondria through the mitophagy pathway (Romanello and Sandri, 2016) are altered in older fibers. Indeed, the expression of proteins involved in mitochondrial fusion, such as mitofusin 2 (MFN2) and the dynamin-like protein OPA1, strongly declined. The decrease in OPA1 was larger for fast 2A fibers, which also show a net increase in the expression of the metalloproteinase OMA1. This dynamic can be explained by the fact that OMA1 cleaves and inactivates OPA1 (Head et al., 2009). Older muscle fibers of both types consistently increase the expression of autophagic adaptors (p62/SQSTM and optineurin [OPTN]) and other autophagy-related genes (GABARAPL2 and BNIP3). Mitochondrial proteostasis and fission also show age-dependent changes (Figure 4B). The expression of a recently identified component of the mitochondrial fission machinery, DNM2 (Lee et al., 2016), clearly increases in aging. Together, these observations show that fission and mitophagy increase in aging, in parallel with the decline in mitochondrial content (Figure 4A).

Mitochondrial oxidative capacity depends on the abundance of mitochondrial proteins and on their assembly and composition, both of which influence the production of ATP per unit mass of protein. To analyze potential differences in mitochondrial protein composition of younger and older fibers, we normalized by the expression of oxidative phosphorylation (OXPHOS) proteins, which corrects for the observed decline in mitochondrial mass in older fibers (Schiaffino et al., 2015). At a permutation-based FDR using a 5% cutoff, GO-annotated mitochondrial proteins showed no age-related changes in fast 2A fibers. Interestingly, however, the mono-amine oxidase A (MAOA) was expressed at a much lower level in older slow fibers ($p < 10^{-4}$; Figure 4C). This outer mitochondrial membrane enzyme catalyzes the oxidative deamination of biogenic amines, generating reactive oxygen species (ROS). Together with the fact that first-degree relatives of type-2-diabetic patients have a 70% reduced expression of MAOA in skeletal muscle compared to individual with no family history of diabetes, this may point to a role of this enzyme in glucose homeostasis (Elgzyri et al., 2012), which notably declines during aging (Barzilai et al., 2012). Conversely, mitochondria of older slow fibers express GSTP1, a glutathione-S-transferase targeted to the mitochondria (Raza, 2011), and glycine aminotransferase (GATM), which synthesizes a precursor of creatine, more highly.

We also quantitated the expression of all the enzymes of the tricarboxylic acid (TCA) cycle in our single-fiber measurements. The majority of these enzymes were slightly decreased or unchanged in aged fibers, regardless of fiber type (Figures S4A and S4B). However, citrate synthase, aconitase, and isocitrate dehydrogenase showed a small but consistent increase in older fast fibers compared to their younger counterparts. We observed that the expression of IDH2, the isocitrate dehydrogenase isoform catalyzing a nicotinamide adenine dinucleotide phosphate (NADP)-dependent reversible conversion of citrate to alpha-ketoglutarate, was much higher than that of the IDH3 complex, the canonical TCA cycle enzyme. The latter

(B) Selected components of the mitochondrial dynamics and quality control machinery, with the corresponding changes in aging in the two fiber types as indicated. Data are represented as median normalized expression ± SEM.

(C) Changes in the mitochondrial proteome of slow fibers in aging. The expression values of mitochondrial proteins (keyword annotation) were normalized by OXPHOS proteins as a proxy for mitochondrial content.

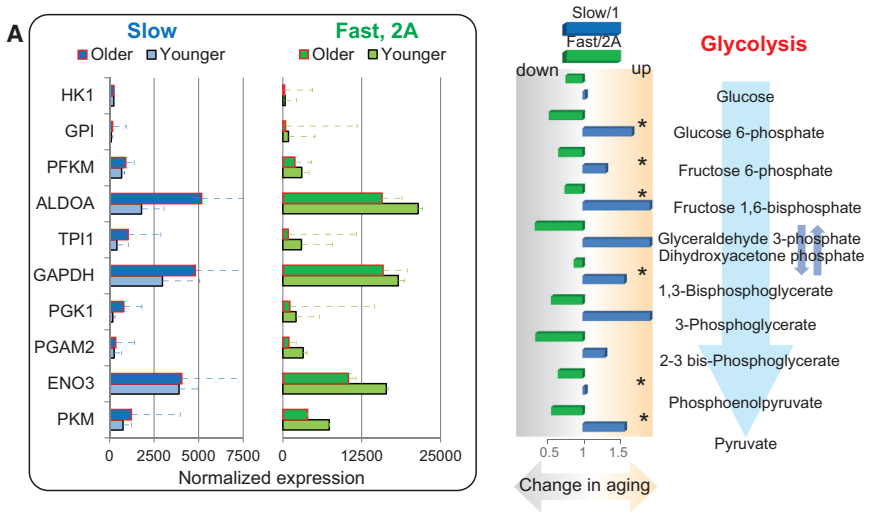

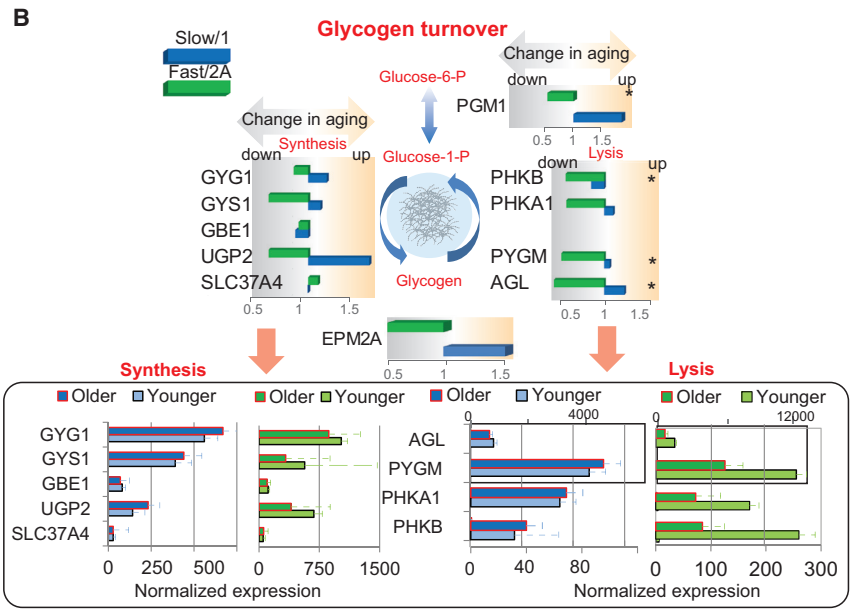

Figure 5. Opposing Changes in Glycolytic and Glycogen Handling Enzymes in Aging Slow and Fast Fibers

(A) Expression of glycolytic enzymes in slow (blue) and fast 2A (green) fibers. Data are represented as median normalized expression ± SEM. The fold change in aging (older/younger ratio) is shown as a bar graph for each enzyme in the two fiber types, with a schematic representation of the corresponding function in the glycolytic pathway.

(B) Schematic representation of a glycogen granule with selected groups of proteins involved in glycogen handling, subdivided by activity type. The median expression change in aging is represented as a bar graph for each fiber type as described above. (*, statistically significant).

catalyzes a NAD-dependent irreversible reaction. The higher abundance of IDH2 than IDH3 in human muscle might explain why individuals with retinitis pigmentosa due to homozygous loss-of-function mutation of *IDH3B* do not have a muscle phenotype, despite the prominent oxidative metabolism characterizing this tissue (Hartong et al., 2008).

Differential Regulation of a Major Axis of Carbohydrate Metabolism during Aging

Glycogen is a fundamental source of carbohydrates for muscle metabolism, especially for fast fibers, which rely more on glycolysis than slow fibers to support the energy demand of their short intense bouts of contraction (Jensen and Richter, 2012; Schiaffino and Reggiani, 2011). The differential response in glycolysis during aging (Figure 3F) prompted us to analyze age-related changes of glycolytic enzymes. As expected, their expression was higher in fast than in slow fibers. Interestingly, the expression of the majority of glycolytic enzymes increased in older slow fibers compared to their young counterparts. In contrast, the same proteins showed a clear decrease in older fast 2A fibers (Figure 5A). A graphic representation of the glycolytic pathways, illustrating the flow of glycolytic substrates and the corresponding enzymes with fold changes in aging, indicates that the difference in the expression of the glycolytic pathway between fiber types fades during aging. In fast 2A/2X fibers, which also express MYH1 and have the fastest contraction parameters and highest glycolytic activity (Schiaffino and Reggiani, 2011), there is an even more pronounced effect, with most of the glycolytic enzymes decreased more than 2-fold (Figure S4C). We confirmed the above analyses normalizing by ACTA1, DMD, and without any normalization (Figures S3 and S4D). DMD normalization yielded similar results to ACTA normalization, whereas in the absence of normalization, the decline in aging fast fibers was even steeper than with normalized values, a likely effect of the observed decrease in size (Figures 1A–1C). Thus, there is a clear increase in glycolytic enzymes in older slow fibers, regardless of analysis procedure.

We next asked whether the proteins involved in glycogen storage and metabolism were also changing in aging in a fiber-type-specific manner. Indeed, slow fibers show a median increase in the expression of enzymes involved in glycogen handling in aging (Figure 5B). In fast 2A fibers, we observed a consistent decrease in the expression of these enzymes, which was even more pronounced in fast 2A/2X fibers, the most glycolytic of the three subtypes (Figure S4E). These changes were most severe for the enzymes involved in glycogen hydrolysis. Glycogenin (GYG1), which initiates

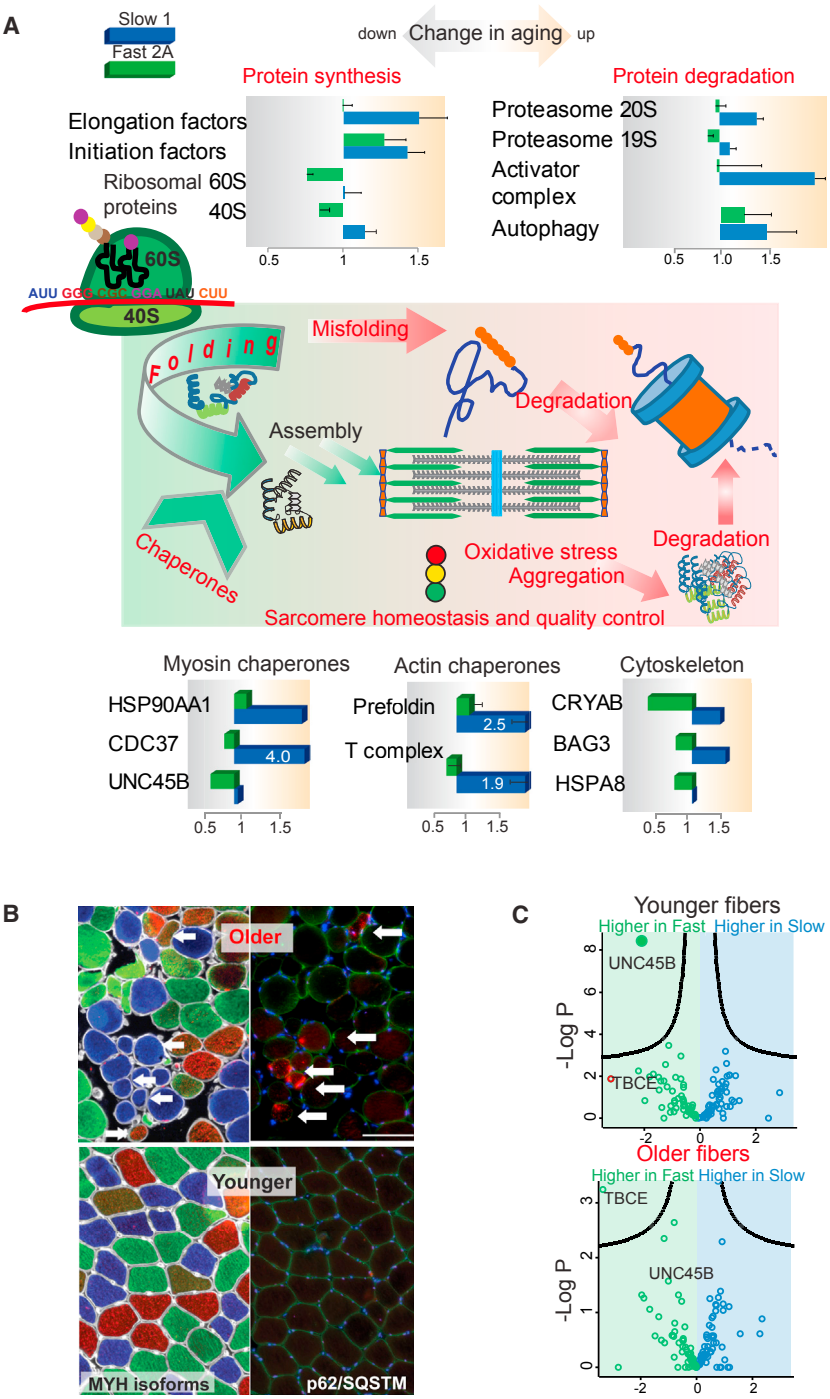

Figure 6. Protein Quality Control in Aging Fast and Slow Fibers

(A) Selected aspects of sarcomere proteostasis, showing the fold change in aging in slow and fast fibers. For multi-protein complexes, data are represented as median change ± SEM; all quantitated components of each complex were analyzed. Ratios that were higher than the scale maximum are reported inside the bars. IF, intermediate filaments.

(B) Immunohistochemistry on sections of muscle biopsies, comparing p62 expression in younger and older muscles. Serial sections were stained with antibodies specific for different isoforms of MYH as in Figure 1A. The bar represents 100 μm.

(C) Volcano plots comparing the expression of chaperones (keyword annotation) in slow and fast 2A fibers.

glycogen assembly and forms the center of the granules, is also reduced in the fast fibers of the older donors. Our data thus suggest that the ability to assemble and utilize glycogen granules is greatly reduced in older fast but unchanged in slow fibers. Thus, fundamental pathways of carbohydrate metabolism change in aging in a fiber-type-specific manner. Given the predominantly glycolytic metabolism of fast fibers, they would be expected to be severely affected by these changes.

Sarcomere Homeostasis and Protein Quality Control in Aging

Unlike slow fibers, fast fibers undergo a significant size reduction in aging (Figures 1B and 1C). Sarcomeres cover more than 90% of muscle fiber volume, and muscle growth and atrophy depend on the rate of sarcomere turnover. We thus set out to investigate potential differences in sarcomere homeostasis in aging slow and fast fibers, focusing on protein synthesis and degradation as well as sarcomeric protein folding, the three main regulators of muscle mass (Figure 6A). This revealed a general upregulation of ribosomal proteins and elongation factors in aging slow fibers, whereas fast 2A fibers showed a downregulation. It is already known that key translation elongation factors are less phosphorylated, and thus more active, in slow compared to fast 2A fibers (Rose et al., 2009). The main components of the proteasomal machinery were upregulated in slow fibers and downregulated or unchanged in fast 2A fibers. Proteins annotated with the keyword autophagy clearly increased in aging in both fiber types, possibly as a protective mechanism counteracting age-induced muscle degeneration (Carnio et al., 2014). To further investigate this, we analyzed the expression of the autophagy marker p62/SQSTM by immunohistochemistry in biopsies of young and older subjects. In serial sections, a clear punctate pattern of p62 expression could only be detected in some biopsies from older donors (Figure 6B). The p62 staining was selective for atrophic fibers of both slow and fast types.

Our observation that slow fibers increase the expression of protein complexes controlling both synthesis and degradation suggests that they are better equipped than fast 2A fibers to sustain the turnover of sarcomeric proteins in aging. In line with this hypothesis, we observed that the expression of individual

chaperones and chaperone complexes that assist folding of the main sarcomeric proteins increases in slow fibers from older individuals but tends to decrease in fast fibers (Figure 6A). This is the case for myosin chaperones like HSP90AA1, its co-chaperone CDC37, and UNC45B. The latter is the mammalian homolog of *C. elegans* Unc-45, a key regulator of paramyosin folding in worm muscle cells. The expression of this muscle-specific chaperone was significantly higher in young fast 2A fibers compared to young slow fibers, but this feature was lost in older fibers, which show little fiber-type-specific difference (Figure 6C). Because this chaperone and its interaction partners are structurally conserved during evolution (Hoppe et al., 2004), a relative decrease in UNC-45B in aging fast human fibers may affect muscle turnover and performance. Interestingly, in aging fast fibers, we observed a reduction in the expression of chaperones and co-chaperones that assist folding of intermediate filaments and the structural assembly of the sarcomere Z line (Figure 6A). The expression of the small heat shock protein alpha B-crystallin (CRYAB), a chaperone for desmin (DES), decreased about 50% in older fast 2A fibers. This protein plays a prominent role in sarcomere stability, as CRYAB mutations cause a dominant form of myofibrillar myopathy, characterized by DES aggregates and progressive muscle weakness (Vicart et al., 1998). In aging fast, but not slow, fibers, we measured a reduction in the expression of HSPA8 and its co-chaperone BAG3, a multi-domain protein that localizes to the Z disk and controls its assembly (Hishiya et al., 2010). Mutations in this co-chaperone also cause a severe, dominant form of myofibrillar myopathy and intracellular aggregates containing DES. A small decrease in the Z disk proteins DES and ZASP/LDB3 was evident in older fast, but not slow, fibers, whereas the expression of myotilin (MYOT) and plectin (PLEC) decreased in both fiber types (Figure S5A). Mutations in these structural proteins cause myopathies with disintegration of the Z disk. We therefore looked for desmin aggregates that characterize myofibrillar myopathies in muscles from our older donor cohort but did not find clear evidence of them, even in the fibers that were positive for the autophagic marker p62 (Figure S5B). Thus, the fiber-type-specific changes in the expression of CRYAB and other Z disk protein chaperones show that the turnover and quality control of sarcomeric proteins tend to decline in aging, though in a milder form than in the overtly pathological context of myopathies.

DISCUSSION

Like all other tissues, muscles are made up of specialized functional units. Their single cell types are the slow and fast fibers, which along with their different contractile properties also have different substrate utilization and general metabolic features. Ideally, these functional units should be studied individually in dynamic contexts, such as disease or aging. At the transcript level, the ongoing revolution in deep sequencing technology is making this aspiration a reality in many different contexts (Jaitin et al., 2014; Tang et al., 2009). Analysis of the proteome is technologically much more challenging, and single-cell proteomics has remained out of reach so far. Here, building on recent advances in proteomics technology in our laboratory in the analysis of muscle (Deshmukh et al., 2015; Murgia et al., 2015), we demonstrate the analysis of single human muscle fibers in the context of aging. By selecting healthy and physically active donors of two widely spaced age groups, we focused on the changes in muscle structure and function at the proteome level, which occur as consequence of aging, irrespective of muscle disuse.

Our streamlined, single-shot workflow allowed the analysis of a relatively large number of muscle proteomes—152 single fibers from eight donors. These results included isoform-specific quantitation of myosin, which immediately classifies them into fiber types. We found that a large majority of fibers were of a pure type and less than 20% express two myosin isoforms at comparable levels. Despite the extremely challenging dynamic range of muscle, the single fiber results were sufficient to quantify the contractile apparatus, the sarcoplasmic reticulum, which couples membrane depolarization to filament movement, and the respiratory chain essentially to completion. Age-related sarcopenia strongly affects fast, but not slow, fibers in humans (Andersen, 2003; Lexell, 1995), but the molecular basis for this observation remains unknown at the proteome level. We here show that slow and fast muscle fibers undergo diverging metabolic changes in aging. Single-fiber proteomics was instrumental in this, because we observed not only differential but often opposing behaviors, which would have been attenuated or completely obscured at the tissue level.

Our results clearly show that many glycolytic enzymes are expressed at significantly higher levels in the slow fibers of our older donor cohort compared to their younger counterpart (Figure 5). In stark contrast, the same enzymes show a sharp age-related decline in expression in the fast fibers. This was especially pronounced in the type 2A/2X, the fastest fiber type investigated. The enzyme system responsible for glycogen hydrolysis and granule synthesis followed precisely the same pattern, unambiguously involving carbohydrate metabolism in fiber-type-specific aging. Glycogen is a fundamental source of carbohydrates for muscle metabolism, and its depletion severely affects muscle performance, leading to fatigue (Ørtenblad et al., 2013). It is well known that fast fibers have higher glycogen content than their slow counterparts. Indeed, depletion of muscle glycogen has been reported in the vastus lateralis of older compared to young subjects (Meredith et al., 1989). Whereas our results are in line with previous reports in whole muscles and in single isolated fibers (Albers et al., 2015), proteomics now quantitates the molecular basis of these observations directly at the level of the members of the relevant pathways. Because post-translational modifications additionally modulate enzymatic activity, it would be interesting to expand proteomic analysis into this area as technology advances.

We observed a decrease in mitochondrial content in both fast and slow older fibers in line with a large number of previous studies (Johnson et al., 2013; Ljubicic and Hood, 2009). Intriguingly, this was paralleled by a concomitant increase in the mitophagy pathway and decrease in the fusion machinery, two mechanisms that may at least partly explain age-related mitochondrial defects. Normalization by OXPHOS proteins as a proxy for mitochondrial content revealed changes in

mitochondrial composition in aging and specifically a several-fold decrease of MAOA in slow fibers. This mitochondrial outer membrane enzyme catalyzes the oxidative deamination of biogenic amines, generating reaction byproducts that increase oxidative stress and associated cellular responses. The oxidation of the dietary amine tyramine by MAOA stimulates glucose uptake in skeletal muscle and adipocytes by acting on GLUT4 translocation (Morin et al., 2002); thus, the decreased expression of MAOA in the slow fibers of skeletal muscle may contribute to age-associated glucose intolerance. This is further supported by the recent observation that first-degree relatives of type 2 diabetic patients have a 70% reduced expression of MAOA in skeletal muscle compared to an individual with no family history of diabetes (Elgzyri et al., 2012).

A large part of the energetic demands of skeletal muscle fibers is devoted to contraction, especially to the actin-myosin motor system and to the generation and maintenance of concentration gradients across the membranes. Additionally, muscle fibers have energetic requirements for controlling sarcomere turnover, similarly to the requirements for growth and division of proliferating cells but focused on protein synthesis. Our proteomics results indicate that the loss of mitochondrial function in both fiber types is only compensated by increasing the capacity for carbohydrate metabolism in slow fibers. Because we already normalized for the smaller cross sections of older fast fibers (Figures 1A–1C), the decrease in glycolytic capability compared to older slow fibers is even greater. Furthermore, complexes involved in protein synthesis and folding specifically decline in fast fibers. Whereas glycolysis is inefficient compared to oxidative phosphorylation in terms of ATP production per molecule of glucose, its intermediates can be diverted to macromolecular precursors of nucleotides, amino acids, and fatty acids to sustain muscle growth (Vander Heiden et al., 2011). We thus hypothesize that a relative upregulation of glycolysis, by increasing the availability of carbon intermediates, could be one of the muscle-autonomous mechanisms whereby slow muscle fibers sustain protein synthesis as they age. In support of our hypothesis, the expression of phosphoglycerate kinase 1 (PGK1), the first ATP-generating enzyme in the glycolytic pathway is 4-fold higher in older than in younger slow fibers but 2-fold lower in older fast fibers. This enzyme is upregulated in many human cancers and has recently been shown to translocate to the mitochondria, where it specifically phosphorylates pyruvate dehydrogenase kinase (PDHK). The net effect of this interaction is to divert pyruvate from the TCA cycle through the inhibition of pyruvate dehydrogenase, promoting the conversion to lactate and further biosynthetic intermediates (Li et al., 2016). This metabolic remodeling of slow fibers could contribute to maintain an adequate rate of protein synthesis, contributing to the positive effects of exercise and protein intake. These lifestyle interventions lead to an increase of muscle mass in the elderly, but secondary factors like decreased amino acid absorption may contribute to anabolic resistance (Burd et al., 2013). The biosynthesis of amino acids from glycolytic intermediates could thus be an additional player in maintaining protein balance in aging. Supporting our overall view, reversing the age-related loss of mass in fast fibers restores some of their functionality and counteracts whole-body decline in aging mice (Akasaki et al., 2014).

The notion that protein synthesis and turnover are more active in older slow than fast fibers is supported by our results, as slow fibers have more ribosomes and a higher expression of proteasome subunits per volume unit (Figure 6). Measurements of protein fractional synthesis rates in isolated human muscle fibers further sustain this assessment (Dickinson et al., 2010). A decrease in proteasome activity is a feature of aging and disease, and proteasome inhibition causes senescence in various cell models because this proteolytic system plays a major role in quality control of the cellular proteome by removing abnormally folded and damaged proteins (Chondrogianni et al., 2008; Vilchez et al., 2014). Furthermore, the older slow fibers also expressed myosin and actin chaperones at a higher level than the corresponding fast fibers, presumably assisting the complex assembly of contractile proteins subjected to the stress of the continuous contractile activity typical of slow muscle fibers. In addition, we observed a decline in the expression of CRYAB and other chaperones and structural proteins that localize to the Z line of the sarcomere. Because mutations in these proteins can cause dominant forms of myofibrillar myopathies, an adequate expression level of these proteins is likely crucial for sarcomere stability. In addition, dysfunction of CRYAB and Z disk proteins are associated with a reduction in mitochondrial mass and respiratory chain deficiencies (Vincent et al., 2016). Thus, changes in the expression of chaperones and Z disk proteins may directly contribute to the mitochondrial decline that we observed in aging fibers. Altogether, our proteomic investigation demonstrates that several of the main mechanisms responsible for sarcomere homeostasis are differently regulated during aging in slow and fast fibers. By extension, the combination of a higher rate of protein synthesis with more efficient quality control mechanisms and folding in slow fibers may make them be better equipped for counteracting the environmental and metabolic features that drive dysfunction in aging muscle. Sarcopenia in older adults involves primarily fast muscle fibers, as slow fibers are engaged in tonic postural activity, which tends to be maintained even when mobility decreases. Targeted interventions aimed specifically at the pathways involved in age-related decline of fast fibers may therefore be particularly beneficial in counteracting muscle-related frailty in the elderly.

EXPERIMENTAL PROCEDURES

Single Fibers Sample Processing

Fibers were lysed in 10 μL of a solution containing sodium deoxycholate (SDC) reduction and alkylation buffer (Kulak et al., 2014; Murgia et al., 2015). Fiber lysates were boiled for 5 min and sonicated in a water-bath sonicator (Diagenode) for 15 min with a 50% duty cycle. After cooling to room temperature, 10 μL of 100 mM Tris (pH 8.5) was added, followed by 500 ng of endoproteinase LysC, and incubated at 25°C for 3 hr under continuous stirring. Trypsin (400 ng) was added, and the digestion was carried out at 37°C overnight. Peptides from each fiber were acidified to a final concentration of 0.1% trifluoroacetic acid (TFA) and loaded onto StageTip plugs of styrene divinylbenzene reversed-phase sulfonate (SDB-RPS). Purified peptides were eluted with 80% acetonitrile-1% ammonia and dried.

Liquid Chromatography and MS

Peptides were separated on 50-cm columns of ReproSil-Pur C18-AQ 1.9-μm resin (Dr. Maisch) packed in house. The columns were kept at 55°C using a column oven controlled by the SprayQC software (Scheltema and Mann, 2012).

Liquid chromatography performed on an EASY-nLC 1200 ultra-high pressure system was coupled through a nanoelectrospray source to a Q Exactive HF mass spectrometer (all from Thermo Fisher Scientific). Peptides were loaded in buffer A (0.1% [v/v] formic acid), applying a nonlinear 120-min gradient of 2%–60% buffer B (0.1% [v/v] formic acid and 80% [v/v] acetonitrile) at a flow rate of 250 nL/min. Data acquisition switched between a full scan and ten data-dependent MS/MS scans. Multiple sequencing of peptides was minimized by excluding the selected peptide candidates for 30 s.

Computational Proteomics

The MaxQuant software (version 1.5.3.34) was used for the analysis of raw files, and peak lists were searched against the human UniProt FASTA reference proteomes version of 2016 and a common contaminants database by the Andromeda search engine (Cox and Mann, 2008; Cox et al., 2011). The FDR was set to 1% for peptides (minimum length of seven amino acids) and proteins and was determined by searching a reverse database. A maximum of three missed cleavages were allowed in the database search. Peptide identification was performed with an initial allowed precursor mass deviation up to 7 ppm and an allowed fragment mass deviation 20 ppm. Two single fibers with less than 1,000 quantified proteins were excluded from the analysis. For MYH isoforms quantification, only peptides unique to each isoform were used for quantification in MaxQuant.

Bioinformatic and Statistical Analysis

Analyses were performed with the Perseus software (version 1.5.4.2), part of the MaxQuant environment (Tyanova et al., 2016). Categorical annotations were supplied in the form of UniProt Keywords, Kyoto Encyclopedia of Genes and Genomes (KEGG), and Gene Ontology. We extracted mitochondrial proteins filtering by the UniProt keyword "mitochondrion". Intensity values normalized by protein length (MaxQuant IBAQ output) were normalized by the value of skeletal actin (ACTA1). The same procedure was adopted for the normalization by DMD. Student's t tests and ANOVA were performed using 0.05 FDR for truncation and 250 randomizations.

Study Participants

Experiments were performed with approval from the Ethics Committee of the University of Padua, Department of Biomedical Sciences (HEC-DSB08/16). Participants provided informed written consent, and the study was performed in accordance with the Declaration of Helsinki. Participants were males of Italian ancestry, non-smokers, engaged in regular physical activity, and living in the same area at sea level.

ACCESSION NUMBERS

The accession number for the mass spectrometry proteomics data reported in this paper is ProteomeXchange: PXD006182.

SUPPLEMENTAL INFORMATION

Supplemental Information includes Supplemental Experimental Procedures, five figures, and six tables and can be found with this article online at http://dx.doi.org/10.1016/j.celrep.2017.05.054.

AUTHOR CONTRIBUTIONS

Conceptualization, M. Murgia, C.R., S.S., and M. Mann; Methodology, M. Murgia and N.N.; Validation, M. Murgia and N.N.; Formal Analysis, M. Murgia, L.T., and S.S.; Investigation, M. Murgia, C.R., L.T., S.C., S.S., and V.V.; Resources, C.R., V.V., S.S., and M. Mann; Writing, M. Murgia and M. Mann; Visualization, M. Murgia and S.C.; Funding Acquisition, M. Mann.

ACKNOWLEDGMENTS

We are grateful to G. Sowa, I. Paron, and K. Mayr for their assistance with MS; to Philipp Geyer for helping with fractionation (all at the MPIB); to A. Moretti (TU München) for the induced pluripotent stem cell (iPSC)-derived muscle cells; to Lina Cancellara (University of Padua) for helping with biopsy analysis; and to the students and colleagues who volunteered for the muscle biopsy. This work was supported by the Max-Planck Society for the Advancement of Science; The Louis Jeantet Foundation; and EU 7th Framework Programme (grant agreement HEALTH-F4-2008-201648/PROSPECTS).

Received: February 17, 2017
Revised: April 10, 2017
Accepted: May 17, 2017
Published: June 13, 2017

REFERENCES

Aebersold, R., and Mann, M. (2016). Mass-spectrometric exploration of proteome structure and function. Nature *537*, 347–355.

Akasaki, Y., Ouchi, N., Izumiya, Y., Bernardo, B.L., Lebrasseur, N.K., and Walsh, K. (2014). Glycolytic fast-twitch muscle fiber restoration counters adverse age-related changes in body composition and metabolism. Aging Cell *13*, 80–91.

Albers, P.H., Pedersen, A.J., Birk, J.B., Kristensen, D.E., Vind, B.F., Baba, O., Nøhr, J., Højlund, K., and Wojtaszewski, J.F. (2015). Human muscle fiber type-specific insulin signaling: impact of obesity and type 2 diabetes. Diabetes *64*, 485–497.

Andersen, J.L. (2003). Muscle fibre type adaptation in the elderly human muscle. Scand. J. Med. Sci. Sports *13*, 40–47.

Barzilai, N., Huffman, D.M., Muzumdar, R.H., and Bartke, A. (2012). The critical role of metabolic pathways in aging. Diabetes *61*, 1315–1322.

Brunner, F., Schmid, A., Sheikhzadeh, A., Nordin, M., Yoon, J., and Frankel, V. (2007). Effects of aging on Type II muscle fibers: a systematic review of the literature. J. Aging Phys. Act. *15*, 336–348.

Buchholz, J.N., Behringer, E.J., Pottorf, W.J., Pearce, W.J., and Vanterpool, C.K. (2007). Age-dependent changes in Ca2+ homeostasis in peripheral neurones: implications for changes in function. Aging Cell *6*, 285–296.

Burd, N.A., Gorissen, S.H., and van Loon, L.J. (2013). Anabolic resistance of muscle protein synthesis with aging. Exerc. Sport Sci. Rev. *41*, 169–173.

Carnio, S., LoVerso, F., Baraibar, M.A., Longa, E., Khan, M.M., Maffei, M., Reischl, M., Canepari, M., Loefler, S., Kern, H., et al. (2014). Autophagy impairment in muscle induces neuromuscular junction degeneration and precocious aging. Cell Rep. *8*, 1509–1521.

Cartee, G.D., Hepple, R.T., Bamman, M.M., and Zierath, J.R. (2016). Exercise promotes healthy aging of skeletal muscle. Cell Metab. *23*, 1034–1047.

Carter, H.N., Chen, C.C., and Hood, D.A. (2015). Mitochondria, muscle health, and exercise with advancing age. Physiology (Bethesda) *30*, 208–223.

Chemello, F., Bean, C., Cancellara, P., Laveder, P., Reggiani, C., and Lanfranchi, G. (2011). Microgenomic analysis in skeletal muscle: expression signatures of individual fast and slow myofibers. PLoS ONE *6*, e16807.

Chondrogianni, N., Trougakos, I.P., Kletsas, D., Chen, Q.M., and Gonos, E.S. (2008). Partial proteasome inhibition in human fibroblasts triggers accelerated M1 senescence or M2 crisis depending on p53 and Rb status. Aging Cell *7*, 717–732.

Conjard, A., and Pette, D. (1999). Phosphocreatine as a marker of contractile activity in single muscle fibres. Pflugers Arch. *438*, 278–282.

Cox, J., and Mann, M. (2008). MaxQuant enables high peptide identification rates, individualized p.p.b.-range mass accuracies and proteome-wide protein quantification. Nat. Biotechnol. *26*, 1367–1372.

Cox, J., Neuhauser, N., Michalski, A., Scheltema, R.A., Olsen, J.V., and Mann, M. (2011). Andromeda: a peptide search engine integrated into the MaxQuant environment. J. Proteome Res. *10*, 1794–1805.

Cox, J., Hein, M.Y., Luber, C.A., Paron, I., Nagaraj, N., and Mann, M. (2014). Accurate proteome-wide label-free quantification by delayed normalization and maximal peptide ratio extraction, termed MaxLFQ. Mol. Cell. Proteomics *13*, 2513–2526.

Deschenes, M.R. (2004). Effects of aging on muscle fibre type and size. Sports Med. *34*, 809–824.

Deshmukh, A.S., Murgia, M., Nagaraj, N., Treebak, J.T., Cox, J., and Mann, M. (2015). Deep proteomics of mouse skeletal muscle enables quantitation of protein isoforms, metabolic pathways, and transcription factors. Mol. Cell. Proteomics *14*, 841–853.

Dickinson, J.M., Lee, J.D., Sullivan, B.E., Harber, M.P., Trappe, S.W., and Trappe, T.A. (2010). A new method to study in vivo protein synthesis in slow- and fast-twitch muscle fibers and initial measurements in humans. J. Appl. Physiol. *108*, 1410–1416.

Drexler, H.C.A., Ruhs, A., Konzer, A., Mendler, L., Bruckskotten, M., Looso, M., Günther, S., Boettger, T., Krüger, M., and Braun, T. (2012). On marathons and sprints: an integrated quantitative proteomics and transcriptomics analysis of differences between slow and fast muscle fibers. Mol. Cell. Proteomics *11*, M111.010801.

Elgzyri, T., Parikh, H., Zhou, Y., Dekker Nitert, M., Rönn, T., Segerström, A.B., Ling, C., Franks, P.W., Wollmer, P., Eriksson, K.F., et al. (2012). First-degree relatives of type 2 diabetic patients have reduced expression of genes involved in fatty acid metabolism in skeletal muscle. J. Clin. Endocrinol. Metab. *97*, E1332–E1337.

Fraterman, S., Zeiger, U., Khurana, T.S., Wilm, M., and Rubinstein, N.A. (2007). Quantitative proteomics profiling of sarcomere associated proteins in limb and extraocular muscle allotypes. Mol. Cell. Proteomics *6*, 728–737.

Gilli, F., Lindberg, R.L., Valentino, P., Marnetto, F., Malucchi, S., Sala, A., Capobianco, M., di Sapio, A., Sperli, F., Kappos, L., et al. (2010). Learning from nature: pregnancy changes the expression of inflammation-related genes in patients with multiple sclerosis. PLoS ONE *5*, e8962.

Grimby, G. (1995). Muscle performance and structure in the elderly as studied cross-sectionally and longitudinally. J. Gerontol. A Biol. Sci. Med. Sci. *50*, 17–22.

Harrison, B.C., Allen, D.L., and Leinwand, L.A. (2011). IIb or not IIb? Regulation of myosin heavy chain gene expression in mice and men. Skelet. Muscle *1*, 5.

Hartong, D.T., Dange, M., McGee, T.L., Berson, E.L., Dryja, T.P., and Colman, R.F. (2008). Insights from retinitis pigmentosa into the roles of isocitrate dehydrogenases in the Krebs cycle. Nat. Genet. *40*, 1230–1234.

Head, B., Griparic, L., Amiri, M., Gandre-Babbe, S., and van der Bliek, A.M. (2009). Inducible proteolytic inactivation of OPA1 mediated by the OMA1 protease in mammalian cells. J. Cell Biol. *187*, 959–966.

Hishiya, A., Kitazawa, T., and Takayama, S. (2010). BAG3 and Hsc70 interact with actin capping protein CapZ to maintain myofibrillar integrity under mechanical stress. Circ. Res. *107*, 1220–1231.

Hood, D.A., Tryon, L.D., Carter, H.N., Kim, Y., and Chen, C.C. (2016). Unravelling the mechanisms regulating muscle mitochondrial biogenesis. Biochem. J. *473*, 2295–2314.

Hoppe, T., Cassata, G., Barral, J.M., Springer, W., Hutagalung, A.H., Epstein, H.F., and Baumeister, R. (2004). Regulation of the myosin-directed chaperone UNC-45 by a novel E3/E4-multiubiquitylation complex in C. elegans. Cell *118*, 337–349.

Irving, B.A., Lanza, I.R., Henderson, G.C., Rao, R.R., Spiegelman, B.M., and Nair, K.S. (2015). Combined training enhances skeletal muscle mitochondrial oxidative capacity independent of age. J. Clin. Endocrinol. Metab. *100*, 1654–1663.

Jaitin, D.A., Kenigsberg, E., Keren-Shaul, H., Elefant, N., Paul, F., Zaretsky, I., Mildner, A., Cohen, N., Jung, S., Tanay, A., and Amit, I. (2014). Massively parallel single-cell RNA-seq for marker-free decomposition of tissues into cell types. Science *343*, 776–779.

Jensen, T.E., and Richter, E.A. (2012). Regulation of glucose and glycogen metabolism during and after exercise. J. Physiol. *590*, 1069–1076.

Johnson, M.L., Robinson, M.M., and Nair, K.S. (2013). Skeletal muscle aging and the mitochondrion. Trends Endocrinol. Metab. *24*, 247–256.

Kent, J.A., and Fitzgerald, L.F. (2016). In vivo mitochondrial function in aging skeletal muscle: capacity, flux and patterns of use. J. Appl. Physiol. *121*, 996–1003.

Kent-Braun, J.A., and Ng, A.V. (1999). Specific strength and voluntary muscle activation in young and elderly women and men. J. Appl. Physiol. *87*, 22–29.

Klitgaard, H., Zhou, M., Schiaffino, S., Betto, R., Salviati, G., and Saltin, B. (1990). Ageing alters the myosin heavy chain composition of single fibres from human skeletal muscle. Acta Physiol. Scand. *140*, 55–62.

Kulak, N.A., Pichler, G., Paron, I., Nagaraj, N., and Mann, M. (2014). Minimal, encapsulated proteomic-sample processing applied to copy-number estimation in eukaryotic cells. Nat. Methods *11*, 319–324.

Kulak, N.A., Geyer, P.E., and Mann, M. (2017). Loss-less nano-fractionator for high sensitivity, high coverage proteomics. Mol. Cell. Proteomics *16*, 694–705.

Landi, F., Cruz-Jentoft, A.J., Liperoti, R., Russo, A., Giovannini, S., Tosato, M., Capoluongo, E., Bernabei, R., and Onder, G. (2013). Sarcopenia and mortality risk in frail older persons aged 80 years and older: results from ilSIRENTE study. Age Ageing *42*, 203–209.

Lanza, I.R., Befroy, D.E., and Kent-Braun, J.A. (2005). Age-related changes in ATP-producing pathways in human skeletal muscle in vivo. J. Appl. Physiol. *99*, 1736–1744.

Lee, J.E., Westrate, L.M., Wu, H., Page, C., and Voeltz, G.K. (2016). Multiple dynamin family members collaborate to drive mitochondrial division. Nature *540*, 139–143.

Lexell, J. (1995). Human aging, muscle mass, and fiber type composition. J. Gerontol. A Biol. Sci. Med. Sci. *50*, 11–16.

Li, X., Jiang, Y., Meisenhelder, J., Yang, W., Hawke, D.H., Zheng, Y., Xia, Y., Aldape, K., He, J., Hunter, T., et al. (2016). Mitochondria-translocated PGK1 functions as a protein kinase to coordinate glycolysis and the TCA cycle in tumorigenesis. Mol. Cell *61*, 705–719.

Ljubicic, V., and Hood, D.A. (2009). Diminished contraction-induced intracellular signaling towards mitochondrial biogenesis in aged skeletal muscle. Aging Cell *8*, 394–404.

Meredith, C.N., Frontera, W.R., Fisher, E.C., Hughes, V.A., Herland, J.C., Edwards, J., and Evans, W.J. (1989). Peripheral effects of endurance training in young and old subjects. J. Appl. Physiol. *66*, 2844–2849.

Morin, N., Visentin, V., Calise, D., Marti, L., Zorzano, A., Testar, X., Valet, P., Fischer, Y., and Carpéné, C. (2002). Tyramine stimulates glucose uptake in insulin-sensitive tissues in vitro and in vivo via its oxidation by amine oxidases. J. Pharmacol. Exp. Ther. *303*, 1238–1247.

Murgia, M., Nagaraj, N., Deshmukh, A.S., Zeiler, M., Cancellara, P., Moretti, I., Reggiani, C., Schiaffino, S., and Mann, M. (2015). Single muscle fiber proteomics reveals unexpected mitochondrial specialization. EMBO Rep. *16*, 387–395.

Ørtenblad, N., Westerblad, H., and Nielsen, J. (2013). Muscle glycogen stores and fatigue. J. Physiol. *591*, 4405–4413.

Payne, A.M., Jimenez-Moreno, R., Wang, Z.M., Messi, M.L., and Delbono, O. (2009). Role of Ca2+, membrane excitability, and Ca2+ stores in failing muscle contraction with aging. Exp. Gerontol. *44*, 261–273.

Raza, H. (2011). Dual localization of glutathione S-transferase in the cytosol and mitochondria: implications in oxidative stress, toxicity and disease. FEBS J. *278*, 4243–4251.

Romanello, V., and Sandri, M. (2016). Mitochondrial quality control and muscle mass maintenance. Front. Physiol. *6*, 422.

Rose, A.J., Bisiani, B., Vistisen, B., Kiens, B., and Richter, E.A. (2009). Skeletal muscle eEF2 and 4EBP1 phosphorylation during endurance exercise is dependent on intensity and muscle fiber type. Am. J. Physiol. Regul. Integr. Comp. Physiol. *296*, R326–R333.

Scheltema, R.A., and Mann, M. (2012). SprayQc: a real-time LC-MS/MS quality monitoring system to maximize uptime using off the shelf components. J. Proteome Res. *11*, 3458–3466.

Scheltema, R.A., Hauschild, J.P., Lange, O., Hornburg, D., Denisov, E., Damoc, E., Kuehn, A., Makarov, A., and Mann, M. (2014). The Q Exactive HF, a Benchtop mass spectrometer with a pre-filter, high-performance quadrupole and an ultra-high-field Orbitrap analyzer. Mol. Cell. Proteomics *13*, 3698–3708.

Schiaffino, S., and Reggiani, C. (2011). Fiber types in mammalian skeletal muscles. Physiol. Rev. *91*, 1447–1531.

Schiaffino, S., Reggiani, C., Kostrominova, T.Y., Mann, M., and Murgia, M. (2015). Mitochondrial specialization revealed by single muscle fiber proteomics: focus on the Krebs cycle. Scand. J. Med. Sci. Sports *25* (*Suppl 4*), 41–48.

Schwanhäusser, B., Busse, D., Li, N., Dittmar, G., Schuchhardt, J., Wolf, J., Chen, W., and Selbach, M. (2011). Global quantification of mammalian gene expression control. Nature *473*, 337–342.

Short, K.R., Bigelow, M.L., Kahl, J., Singh, R., Coenen-Schimke, J., Raghavakaimal, S., and Nair, K.S. (2005). Decline in skeletal muscle mitochondrial function with aging in humans. Proc. Natl. Acad. Sci. USA *102*, 5618–5623.

Tang, F., Barbacioru, C., Wang, Y., Nordman, E., Lee, C., Xu, N., Wang, X., Bodeau, J., Tuch, B.B., Siddiqui, A., et al. (2009). mRNA-seq whole-transcriptome analysis of a single cell. Nat. Methods *6*, 377–382.

Tyanova, S., Temu, T., Sinitcyn, P., Carlson, A., Hein, M.Y., Geiger, T., Mann, M., and Cox, J. (2016). The Perseus computational platform for comprehensive analysis of (prote)omics data. Nat. Methods *13*, 731–740.

Vander Heiden, M.G., Lunt, S.Y., Dayton, T.L., Fiske, B.P., Israelsen, W.J., Mattaini, K.R., Vokes, N.I., Stephanopoulos, G., Cantley, L.C., Metallo, C.M., and Locasale, J.W. (2011). Metabolic pathway alterations that support cell proliferation. Cold Spring Harb. Symp. Quant. Biol. *76*, 325–334.

Vicart, P., Caron, A., Guicheney, P., Li, Z., Prévost, M.C., Faure, A., Chateau, D., Chapon, F., Tomé, F., Dupret, J.M., et al. (1998). A missense mutation in the alphaB-crystallin chaperone gene causes a desmin-related myopathy. Nat. Genet. *20*, 92–95.

Vilchez, D., Saez, I., and Dillin, A. (2014). The role of protein clearance mechanisms in organismal ageing and age-related diseases. Nat. Commun. *5*, 5659.

Vincent, A.E., Grady, J.P., Rocha, M.C., Alston, C.L., Rygiel, K.A., Barresi, R., Taylor, R.W., and Turnbull, D.M. (2016). Mitochondrial dysfunction in myofibrillar myopathy. Neuromuscul. Disord. *26*, 691–701.

Williams, K.E., Miroshnychenko, O., Johansen, E.B., Niles, R.K., Sundaram, R., Kannan, K., Albertolle, M., Zhou, Y., Prasad, N., Drake, P.M., et al. (2015). Urine, peritoneal fluid and omental fat proteomes of reproductive age women: Endometriosis-related changes and associations with endocrine disrupting chemicals. J. Proteomics *113*, 194–205.